

$-2r(\text{P}) = 0.33 \text{ \AA}$),²³ and so this does not necessarily weaken the superexchange interaction. However, the small difference in the distances of the Cr(2)-O-Cr(1)-O-Cr(2) pathway will result in this interaction being weaker in $\alpha\text{-CrAsO}_4$ than in $\alpha\text{-CrPO}_4$. Hence, the differences in the magnetic structures of $\alpha\text{-CrPO}_4$ and $\alpha\text{-CrAsO}_4$ can be attributed to this indirect effect of the Cr-O distances being slightly longer in the latter material, rather than superexchange through the arsenate group being any stronger than that through phosphate.

The presence of antiferromagnetic and weaker ferromagnetic Cr-O-Cr interactions accounts for the magnetic susceptibility variations of these materials. The frustrations due to the competing superexchange pathways result in large $|\theta/T_N|$ ratios although the magnetic ordering has three-dimensional characteristics. Antiferromagnetic Curie-Weiss behavior is observed when $T \gg T_N$, but as $T \rightarrow T_N$, there is a rise in the susceptibility due to short-range ferromagnetic order arising from the Cr(1)-O-

Cr(2) interactions. Below T_N there is a rapid decrease in the short-range ferromagnetic order, and the system tends to anti-ferromagnetism as $T \rightarrow 0$. Thus, no field dependence develops below T_N , in contrast to $\beta\text{-CrAsO}_4$,⁵ in which an ordered weak ferromagnetic component was observed by susceptibility measurements over the same field range. This difference may be explained by the magnetic symmetries of the ordered states; both $\alpha\text{-CrPO}_4$ and $\alpha\text{-CrAsO}_4$ belong to P_1 magnetic groups that cannot allow a ferromagnetic component, whereas $\beta\text{-CrAsO}_4$ belongs to a primitive magnetic group that also permits a ferromagnetic component.⁵

Acknowledgment. We are grateful to R. S. McLean for measuring the magnetic susceptibilities and to the SERC for providing a studentship for J.P.A. and neutron facilities. J.P.A. thanks Christ Church, Oxford, for a Junior Research Fellowship.

Registry No. $\alpha\text{-CrPO}_4$, 7789-04-0; $\alpha\text{-CrAsO}_4$, 15070-22-1.

Supplementary Material Available: A table of bond angles in $\alpha\text{-CrPO}_4$ at 2 K and $\alpha\text{-CrAsO}_4$ at 5 K (1 page). Ordering information is given on any current masthead page.

(23) Shannon, R. D. *Acta Crystallogr.* 1976, A32, 751.

Contribution from the Anorganisch-Chemisches Institut der Universität Münster, Wilhelm-Klemm-Strasse 8, D-4400 Münster, FRG, Department of Chemistry and Materials Science Center, Cornell University, Ithaca, New York 14853-1301, and School of Chemistry, University of Hyderabad, P.O. Central University, Hyderabad 500 134, India

The Richness of Structures Available to CpMS_4MCp Complexes

Wolfgang Tremel,^{†,‡} Roald Hoffmann,^{*,§} and Eluvathingal D. Jemmis^{||}

Received April 19, 1988

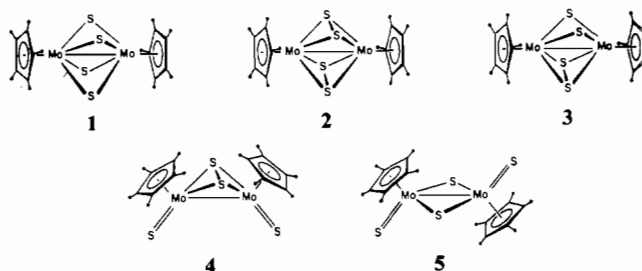
Compounds with the general formula CpMS_4MCp display a remarkable variety in structure. By a detailed theoretical analysis of this class of complexes and related compounds such as NbX_2Y_6 ($X = \text{Se, Te; Y = Br, I}$) or $\text{CpV}(\text{S}_2)_2\text{VCp}$, we are able to explain how the central S_4 unit traverses in many compounds a range in S-S bonding from a ring to isolated sulfide bridges. The isomer $\text{CpMo}(\text{S}_2)_2\text{MoCp}$ can undergo a symmetry-allowed transformation to form $\text{CpMo}(\text{S})\text{S}_2(\text{S})\text{MoCp}$. The bonding in the molecular compounds is compared to that in their solid-state analogues NbX_2Y_6 . As in acetylene complexes, S_2 groups can enter the compounds under study in a parallel and a perpendicular orientation. The latter one is energetically preferred. The rearrangement of parallel- and perpendicular-oriented S_2 groups is symmetry forbidden.

Introduction

The strong affinity of chalcogenides for elements of the transition series is the basis for a variety of metal sulfur compounds. Metal sulfides are the most important class of naturally occurring metal ores.¹ Parallel to this, the chalcogenides display a broad range of capabilities as construction units in the design of stable transition-metal clusters.² Typical goals in this heavily investigated area of inorganic chemistry include the synthesis of models for important biological³ and industrial⁴ catalysts and the preparation of materials for energy storage and conversion.⁵ A particular incentive is the prospect that discrete metal chalcogenide clusters may prove to be functional analogues of the active sites of nitrogenase⁶ and hydrodesulfurization catalysts.⁷

Numerous complexes have been synthesized and structurally characterized, pointing to the extremely versatile ligand behavior of elemental sulfur. It can enter transition-metal compounds in many guises, as sulfide,² disulfide,⁸ or polysulfide.⁹ Each of these sulfur ligands can be linked to several metal atoms. Unsubstituted sulfur, for example, has been reported (besides its occurrence in a terminal position) in doubly,² triply,^{2,10} quadruply,^{10a,11} 5-fold,¹² and 6-fold¹³ bridging geometries.

Given this richness in coordination, it is not surprising that several isomers of the title compound are known. Some of them are shown in 1-5.¹⁴ In structures 1-3 two CpMo fragments are bridged by four S atoms, two of which have transformed into



terminal ligands in 4^{14b} and 5.^{14d} Still more isomers can be thought of. Among those that exist 3^{14c} and 5^{14d} have been structurally

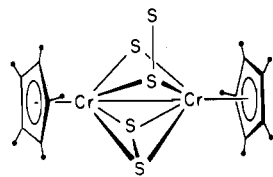
- (1) Vaughn, D. J.; Craig, J. R. *Mineral Chemistry of Metal Sulfides*; Cambridge University Press: Cambridge, U.K., 1978.
- (2) Vahrenkamp, H. *Angew. Chem.* 1975, 87, 363; *Angew. Chem., Int. Ed. Engl.* 1975, 14, 322.
- (3) (a) Coughlin, M. P., Ed. *Molybdenum and Molybdenum Containing Enzymes*; Pergamon Press: Oxford, U.K., 1980. (b) Lovenberg, W., Ed. *Iron Sulfur Proteins*; Academic Press: New York, 1976. (c) Spiro, T. G., Ed. *Iron Sulfur Proteins*; Academic Press: New York, 1982.
- (4) (a) Weisser, O.; Landa, S. *Sulfide Catalysts, Their Properties and Applications*; Pergamon Press: New York, 1973. (b) Gates, B. C.; Katzer, J. R.; Schuit, G. C. A. *Chemistry of Catalytic Processes*; McGraw-Hill: New York, 1979. (c) Bogdanovich, B.; Göttsch, P.; Rubach, M. *J. Mol. Catal.* 1981, 11, 135.
- (5) (a) Tributsch, H. *Ber. Bunsen-Ges. Phys. Chem.* 1977, 81, 361; 1978, 82, 169. (b) Tributsch, H. *J. Electrochem. Soc.* 1978, 125, 169. (c) Tributsch, H. *J. Photochem.* 1985, 29, 89. (d) Tributsch, H. In *Modern Aspects of Electrochemistry*; Bockris, J. O. M.; Conway, B. E., White, R. E., Eds.; Plenum Press: New York, London, 1986; Vol. 17, p 303. (e) Alonso Vante, N.; Jaegermann, W.; Tributsch, H.; Hönl, W.; Yvon, K. *J. Am. Chem. Soc.* 1987, 109, 3251. (f) Ennaoui, A.; Fiechter, S.; Goslowsky, H.; Tributsch, H. *J. Electrochem. Soc.* 1985, 132, 1579.

[†] Liebig-Fellow (1986-1988).

[‡] Universität Münster.

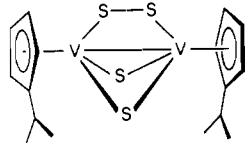
[§] Cornell University.

^{||} University of Hyderabad.



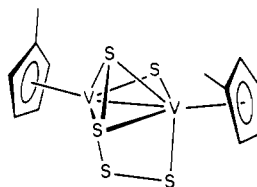
6

attached to the same sulfur atom of a S₂ ligand. Other S₂ coordination modes are known. In (*i*-PrCp)V(S₂)₂V(*i*-PrCp) (7),²⁸



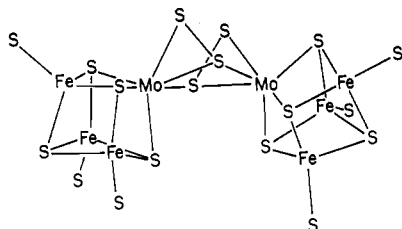
7

we encounter a bridging S₂ group in a parallel orientation; S₂ groups in parallel and perpendicular orientation occur in MeCpV(S₂)₂SVCpMe (8).²⁹ This still does not exhaust the

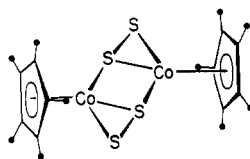


8

variety of S₂ coordination modes, as seen in [Mo₂Fe₆S₈(S₂)₂(SC₆H₄Br)₆]⁴⁻ (9)³⁰ and Me₃CpCo(S₂)₂CoCpMe₅ (10),³¹ where



9

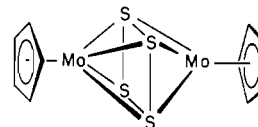


10

the η¹,η²-S₂ ligands are in a steplike syn and anti arrangement, respectively. Many other ways of S₂-bonding are known, and numerous examples can be found in some recent reviews.^{2,8-10}

One way to approach the bonding in the S₄-bridged compounds starts out from a cluster point of view by simply counting electrons. Let us assume CpMoS₄MoCp to be a polyhedral molecule in which the central S₄ ring is sandwiched between two CpMo fragments. Applying the Wade-Mingos³² rules, we find for a completely bonded octahedral M₂X₄ cluster a magic electron count of 46 electrons. This matches exactly the number of cluster electrons in CpMoS₄MoCp. None of the known CpMoS₄MoCp isomers, however, has been reported in this structure type. Instead, the S₄ ring is cleaved in various ways, and the Mo-Mo distances in all structurally characterized isomers are indicative of metal-metal bonds.

In this article we want to explore some of the electronic requirements for stabilizing one or the other isomer of CpMS₄MCp compounds. In particular, we are interested in the early-transition-metal species where M = Mo. We will start out from the hypothetical CpMoS₄MoCp (11). In this model an S₄ ring with

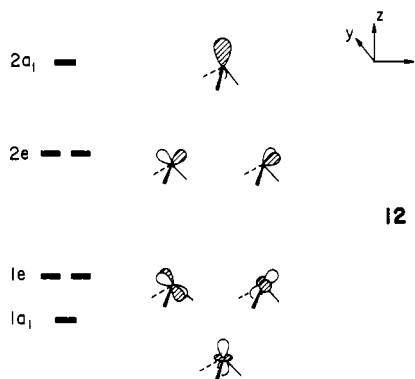


11

normal S-S single-bond distances is sandwiched between two CpMo fragments. It provides a convenient starting point for an analysis. As the S-S distance is stretched (and the Mo-Mo decreases), we will approach structure 1. Further deformation will give 2 and 3. Our conclusions are mainly based on symmetry and overlap arguments supplemented by extended Hückel³³ calculations. The technical details relevant to the computations may be found in the Appendix.

S₄ Rings in the Central Plane

A convenient starting point for the analysis is a fragment approach based on a CpM(X₄)MCp partitioning of the molecule. The orbitals of the isolobal³⁴ conical fragments ML₃ and MCp have been discussed at length elsewhere.³⁵ The basic ordering in energy and the shape of the frontier orbitals of these fragments is shown in 12. At relatively high energy there is an a₁ orbital,



12

- (28) (a) Bolinger, M. C.; Rauchfuss, T. B.; Rheingold, A. L. *J. Am. Chem. Soc.* **1983**, *105*, 6321. The corresponding selenium compound has been reported as well: (b) Rheingold, A. L.; Bolinger, C. M.; Rauchfuss, T. B. *Acta Crystallogr., Sect. C: Cryst. Struct. Commun.* **1986**, *C42*, 1878. Some structurally related Fe and Ru compounds have been reported: (c) [Cp₂Fe₂(S₂(SEt))₂]⁺; Vergamini, P. J.; Ryan, R. R.; Kubas, G. J. *J. Am. Chem. Soc.* **1976**, *98*, 1980. (d) [CpFeS₂]₂; Weberg, R. T.; Haltiwanger, R. C.; Rakowski DuBois, M. *Organometallics* **1985**, *4*, 1315. Weberg, R. T.; Haltiwanger, R. C.; Rakowski DuBois, M. *Nouveau J. Chem.* **1988**, *12*, 361. (e) (C₅Me₄Et)₂Ru₂S₄; Rauchfuss, T. B.; Rodgers, D. P. S.; Wilson, S. R. *J. Am. Chem. Soc.* **1986**, *108*, 3114.
- (29) Bolinger, M. C.; Rauchfuss, T. B.; Rheingold, A. L. *Organometallics* **1982**, *1*, 1551.
- (30) Kovacs, J. A.; Bashkin, J. K.; Holm, R. H. *J. Am. Chem. Soc.* **1985**, *107*, 1784.
- (31) Brunner, H.; Janietz, N.; Meier, W.; Sergeson, G.; Wachter, J.; Zahn, T.; Ziegler, M. L. *Angew. Chem.* **1985**, *97*, 1056; *Angew. Chem., Int. Ed. Engl.* **1985**, *24*, 1060.

- (32) (a) Mingos, D. M. P. *Acc. Chem. Res.* **1984**, *17*, 311. (b) Mingos, D. M. P. In *Comprehensive Organometallic Chemistry*; Wilkinson, G., Stone, F. G. A., Abel, E. W., Eds.; Pergamon Press: Oxford, England, 1981. (c) Mason, R.; Mingos, D. M. P. *MTP Int. Rev. Sci.: Phys. Chem., Ser. Two* **1975**, *11*, 121. (d) Wade, K. *Adv. Inorg. Chem. Radiochem.* **1976**, *18*, 1. (e) Wade, K. *Chem. Br.* **11**, 177. (f) Wade, K. *Inorg. Nucl. Chem. Lett.* **1972**, *8*, 559, 563. (g) Wade, K. *J. Chem. Soc., Chem. Commun.* **1971**, 792. (h) Mingos, D. M. P. *Nature (London), Phys. Sci.* **1972**, *236*, 99. (i) Wade, K. *Electron Deficient Compounds*; Nelson: London, 1971.
- (33) (a) Hoffmann, R.; Lipscomb, W. N. *J. Chem. Phys.* **1962**, *36*, 2179, 3489; **1962**, *37*, 2872. (b) Hoffmann, R. *Ibid.* **1963**, *39*, 1397. (c) Ammeter, J. H.; Bürgi, H.-B.; Thibeault, J. C.; Hoffmann, R. *J. Am. Chem. Soc.* **1978**, *100*, 3686.
- (34) Hoffmann, R. *Angew. Chem.* **1982**, *94*, 725; *Angew. Chem., Int. Ed. Engl.* **1982**, *21*, 711.
- (35) (a) Elian, M.; Hoffmann, R. *Inorg. Chem.* **1975**, *14*, 1058. (b) Burdett, J. K. *Inorg. Chem.* **1975**, *14*, 375. (c) Burdett, J. K. *J. Chem. Soc., Faraday Trans. 2* **1975**, *70*, 1599. (d) Elian, M.; Chen, M. M. L.; Mingos, D. M. P.; Hoffmann, R. *Inorg. Chem.* **1976**, *15*, 1148.

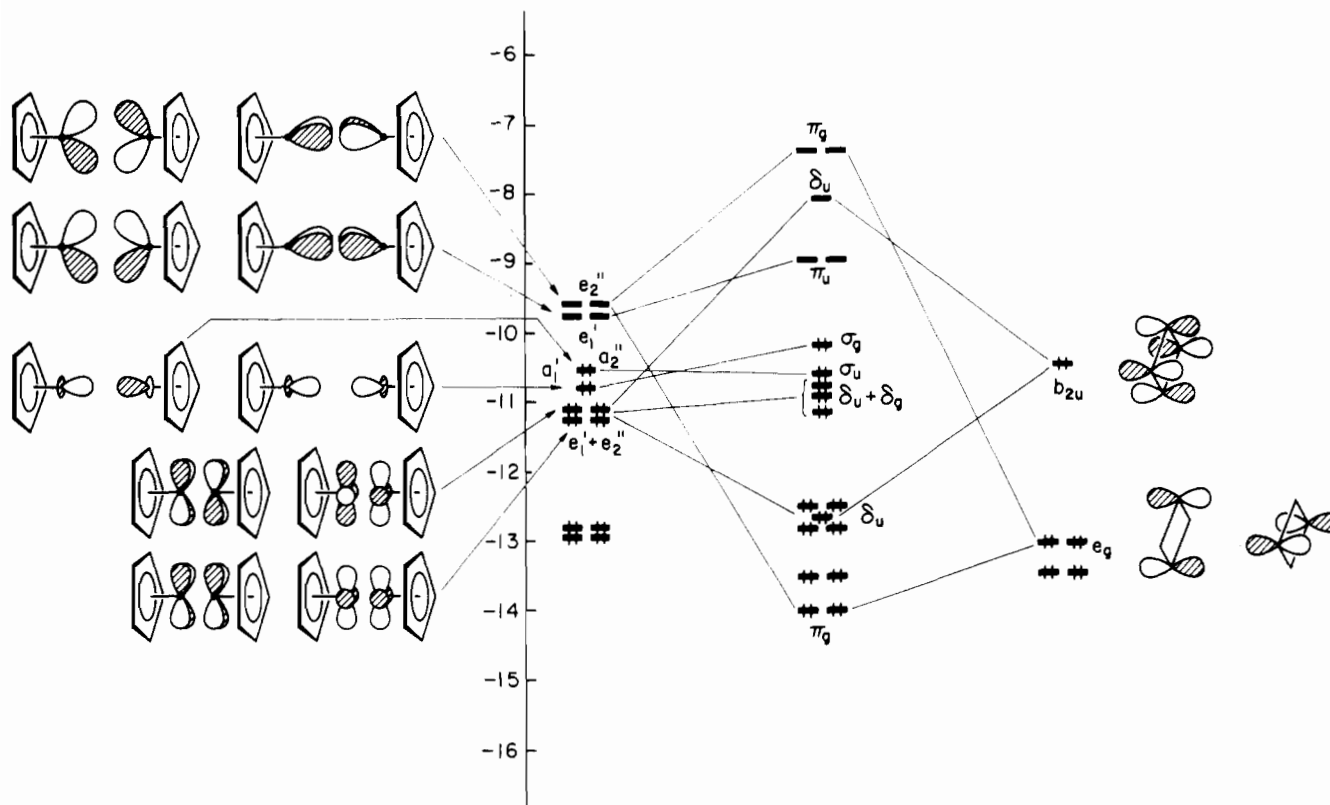


Figure 1. Interaction of two CpMo fragments and *c*-S₄ to form CpMoS₄MoCp.

2a₁, composed of metal s, p and a variable contribution of z² and a 2e set made up of a mixture of metal (xz,yz) and (x,y). These orbitals have the greatest interaction with the bridging ligands.

The lower set of orbitals, which would be the t_{2g} set of non-bonding orbitals in an octahedral metal complex, may be the major source of metal-metal interaction in a dinuclear metal complex of early transition metals. For CpMo the a₁ + e triad is empty and the metal d block (a₁ and e₂) originating primarily from metal z², x²-y², and xy is filled with five electrons. Figure 1 shows the assembly of a computed orbital diagram for the species CpMoS₄MoCp in an idealized C_{2v} (pseudo-D_{4h}) symmetry. The S...S distance in the bridge is fixed at 2.1 Å. On the left are given the orbitals of a CpMo...MoCp dimer. For an Mo-Mo distance of 3.92 Å we find only very small level splittings. For cyclic S₄ we expect to see hydrocarbon-like orbitals interspersed with the sulfur lone pairs.

Our general expectations are fulfilled. The π_g and δ_u orbitals of the composite molecule (D_{∞h} symmetry assumed) are pushed up by the strong interaction between the e₁' and the e₂'' of the S₄ fragment with the symmetry-equivalent combination of the metal dimer. The a₁' and e₂'' orbitals of the metal fragment interact only slightly with the corresponding orbitals of the S₄ ring and stay at approximately the same energy. The result is a nice gap of approximately 1 eV for electron counts of 46 and 50 electrons. Note the high pseudosymmetry D_{∞h} (as indicated by the symmetry labels for the composite molecule in Figure 1); some orbitals are nearly degenerate. On the basis of these considerations, there seems to be nothing wrong with our model compound containing a cyclic S₄ bridging unit. There are, however, except for one recent example, [(η⁵-C₅Me₄Et)Rh(μ,η²-P₂)₂Rh(η⁵-C₅Me₄Et)],³⁶ almost no reports of four-membered rings of group 15 or 16 elements sandwiched between metal fragments.

The structural preferences of our model compound can be probed by varying the Mo-Mo or S...S distances, respectively. Clearly, the variability in these structures and the focus of concern

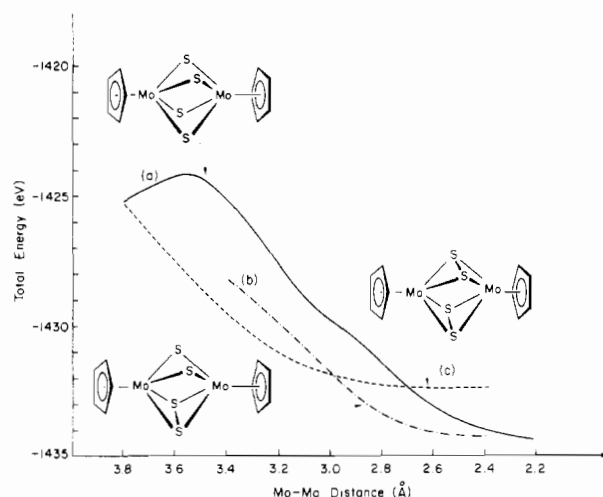


Figure 2. Total energies for three CpMoS₄MoCp isomers as a function of the metal-metal distance: (a) CpMoS₄MoCp; (b) CpMo(S₂)₂MoCp; (c) CpMo(S₂)₂MoCp.

about M-M and S-S bonding lies in the inner octahedron in the bridging region. For this geometry it takes one distance (M-L, M-M, or L-L) and one angle (M-L-M, L-M-L, or M-M-L) or two distances to fix the bridging region. Our model calculations (using a constant Mo-S distance of 2.46 Å) gave a total energy curve as a function of the Mo-Mo distance, as shown in Figure 2. There is a local energy minimum for long Mo-Mo distances in a classic triple-decker type with completely bonded S₄. For increasing S-S and decreasing Mo-Mo distances the energy goes first uphill and then falls to a deep minimum at nonbonding S...S distances and very short Mo-Mo separations. We should point out that total energies cannot be realistically calculated using extended Hückel techniques, especially when there are several crossing orbitals. A good configuration interaction study would be required to establish reliably the existence of a small local minimum.

As a general statement, all S lone-pair orbitals are in energy

(36) Scherer, O. J.; Swarowsky, M.; Wolmershäuser, G. *Angew. Chem.* **1988**, *100*, 423; *Angew. Chem., Int. Ed. Engl.* **1988**, *27*, 416.

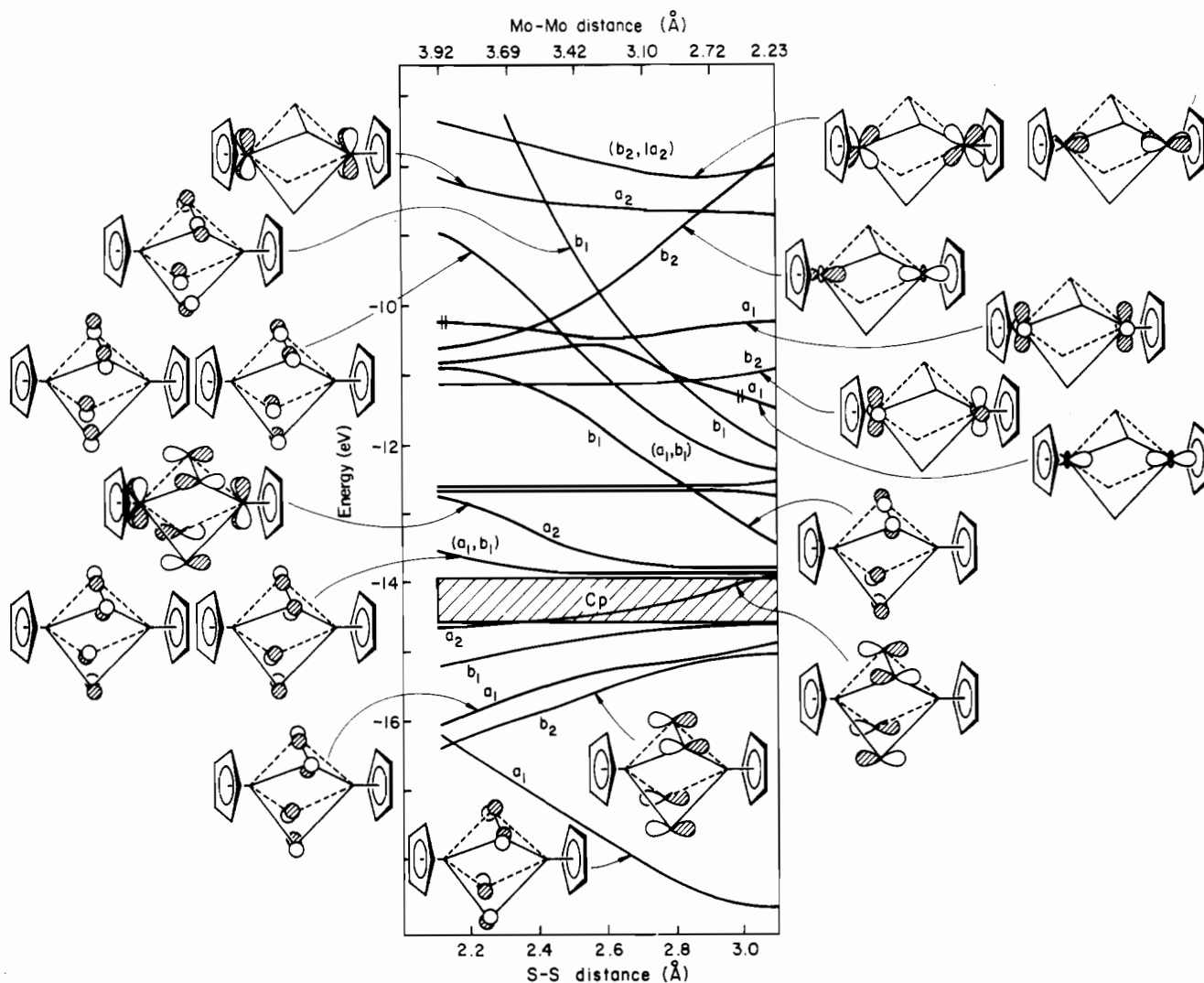
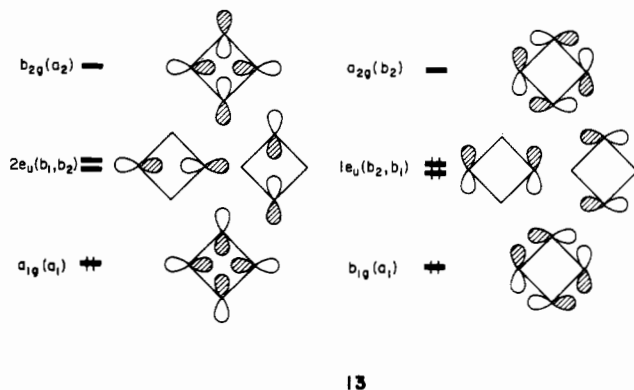


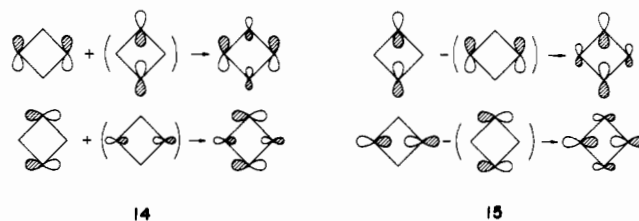
Figure 3. Energy levels of CpMoS₄MoCp as a function of the Mo-Mo distance.

directly below the metal d block for short metal-metal distances. Lengthening the Mo-Mo bond (and decreasing the S...S distances) should stabilize all S-S bonding orbitals and destabilize all antibonding ones. The four-membered S₄ ring has eight in-plane σ orbitals, four radial and four tangential ones, as shown in 13,



with symmetry labels in D_{4h} (C_{2v}) symmetry. The coordinate system in C_{2v} symmetry is chosen with the C_2 axis passing through two S atoms of the S₄ ring, as in Figure 3, in order to obtain a match in symmetry labels. Depending on the S-S separation, there is a variable amount of s,p-mixing, which is neglected in our schematic representation. For short S-S separations we expect the radial a_{1g} (a_1) and tangential b_{1g} (a_1) orbitals to be stabilized. In contrast, the S-S antibonding b_{2g} (b_1) and a_{2g} (b_1) orbitals should be substantially destabilized. The degenerate e_u orbitals

can mix to form one slightly bonding and one slightly antibonding pair, as shown in 14 and 15.



We can identify almost all of these levels in the Walsh diagram in Figure 3. Note again the high cylindrical pseudosymmetry. The a_{1g} ($2a_1$ in Figure 3) and b_{1g} ($1a_1$) orbitals are stabilized for short S-S distances, just as expected. The b_{2g} ($1b_1$) combination of the sulfur s orbitals is raised and ends up right below the p block. One e combination ($3a_1$ and $2b_1$ in Figure 3) is essentially nonbonding and stays at approximately the same energy. The other e combination ($4a_1$ and $4b_1$ in Figure 3), which is antibonding with respect to S-S, is raised high in energy, along with the radial a_{2g} ($5b_1$) orbital. Besides the σ orbitals, for four S atoms we expect to see four π -type orbitals, which—according to the hierarchy of interaction—should be in the “intermediate” energy range and exhibit significantly less dependence on the S-S separation. The all-bonding combination $1b_2$ is lowest in energy (third from bottom). Next we find the nonbonding ($1a_2$, $2b_2$) orbitals. Due to the high pseudosymmetry of the complex they are nearly degenerate. The slight energy spread of the nonbonding pair is caused by mixing in a small amount of metal-metal π^* contribution. This leads to a slight increase in energy for small met-

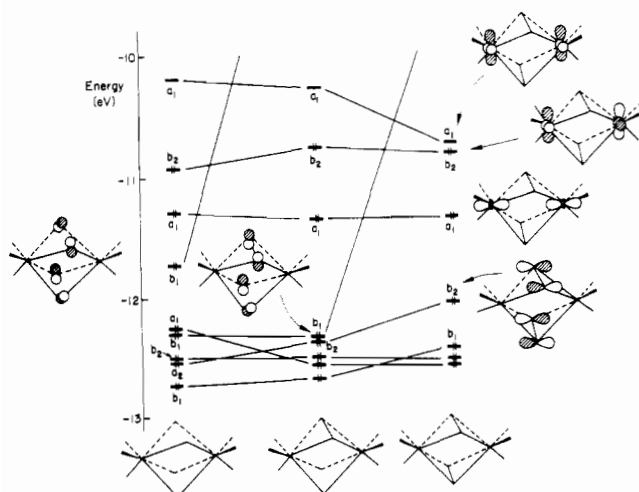
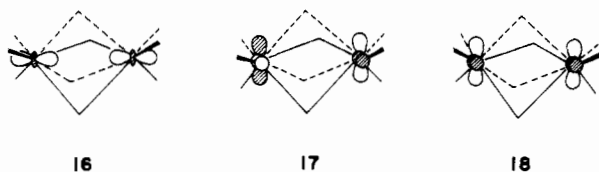


Figure 4. Molecular orbital correlation diagram for the interconversion of three $\text{CpMoS}_4\text{MoCp}$ isomers: (left) $\text{CpMoS}_4\text{MoCp}$; (middle) $\text{CpMo}(\text{S}_2)\text{S}_2\text{MoCp}$; (right) $\text{CpMo}(\text{S}_2)_2\text{MoCp}$.

al-metal distances. At highest energy is the all-antibonding π combination, $2a_2$. As expected, it rises slightly as the S-S distance decreases.

In addition, we have the metal 4d orbitals. For short M-M distances there is the (metal-metal) σ -bonding a_1 orbital **16** ($5a_1$



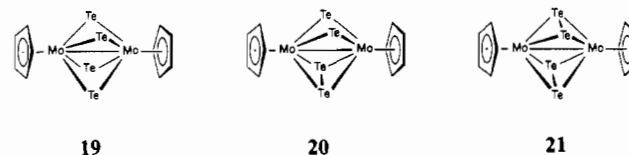
in Figure 3) at lowest energy. Next come the b_2 (δ^*) and a_1 (δ) orbitals **17**, **18** ($3b_2$ and $6a_1$). The other δ/δ^* and the π orbitals are raised higher in energy, due to Mo-Cp interactions. For longer metal-metal distances the metal-metal σ^* -bonding b_2 orbital comes down in energy.

Increasing the Mo-Mo distance (and decreasing the S-S distances) turns on substantial S-S repulsions. Following the Walsh diagram in Figure 3, all S-S antibonding orbitals are

occupied up to a Mo-Mo distance of 3.3 Å. The structure, however, seeks to minimize S-S repulsions. As a consequence, a geometry with a short metal-metal bond and long S-S separations is preferred.

The situation is not much different for **2** and **3**. The total energy change for variation of metal-metal distances is shown in Figure 2b,c. Now we have energy minima at Mo-Mo distances around 2.6 Å, which is close to the observed geometry in **3**. The Walsh diagrams are qualitatively alike in all three cases, and we do not show all of them. We have to be careful about electron book-keeping: replacing two S^{2-} by one S_2^{2-} without changing the charge on the complex results in a formal two-electron reduction of the metals. For **3** and **2**, one or two orbitals, respectively, are out of range in energy, because one or two S-S bonds are formed. **2**, **3**, and **1** are related by a sequence of two-electron reductions. The evolution of the frontier orbitals at a Mo-Mo distance of 2.6 Å for this series is shown schematically in Figure 4. Most of the orbitals experience only minor energy shifts. The b_1 orbitals, however, which are responsible for the bond breaking/making process, are very much affected by the structural change. For each bond formed the uppermost level is raised above the metal d block. Energetically, **3** is favored by approximately 0.5 eV (no geometry optimization); next comes **2** and then **1**. **3** is known, **1** has never been reported, and **2** has been suggested on the basis of spectroscopic data, as we pointed out before. The reason for the stability sequence is likely to be found in the reduced S...S repulsion.

What happens if we have higher group 16 homologues such as Te as bridging atoms? We did a set of calculations on the corresponding Te compounds **19-21** as well (Mo-Te: 2.75 Å).



A Walsh diagram for the variation of the Mo-Mo distance in **19** is given in Figure 5. Replacing S by Te shifts all the formerly S-based levels to higher energies. This is a consequence of the Te 5p orbitals being much more diffuse than S 3p. The increased Te-Te interactions are evidenced by the appearance of the Te-based antibonding b_1 combination above the metal d block. Therefore, in the Te compounds some of the antibonding in-plane

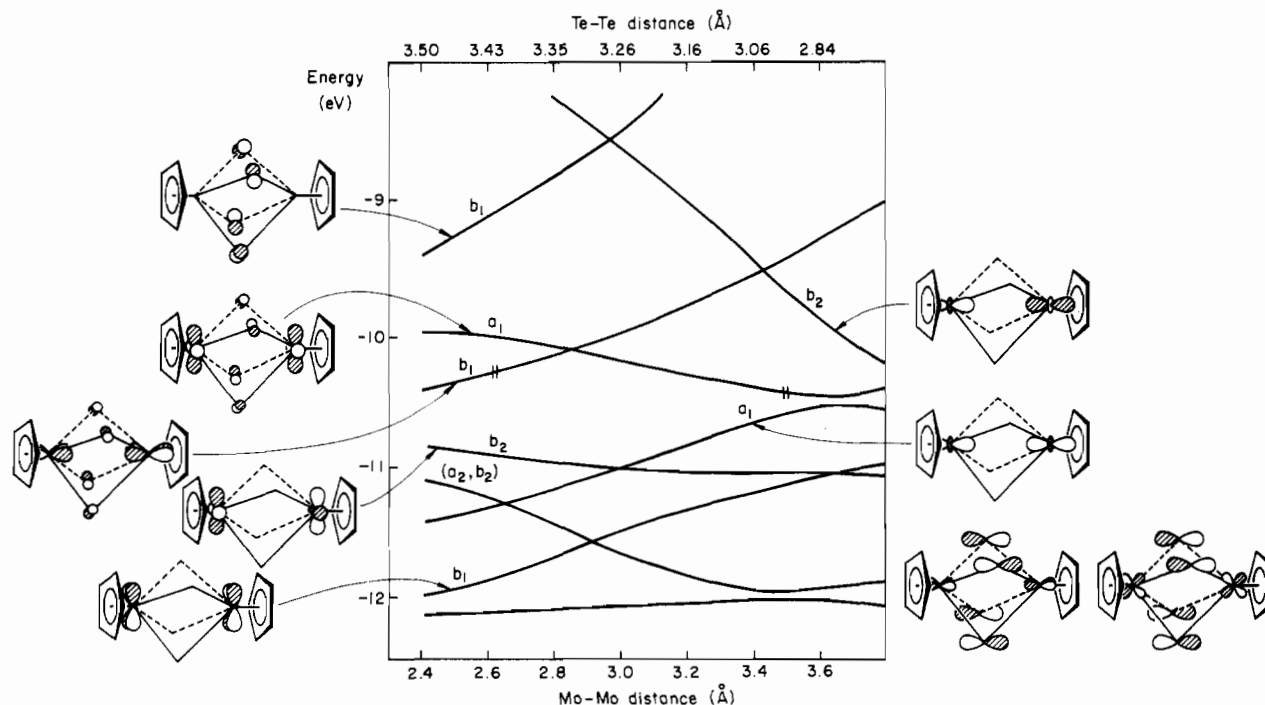


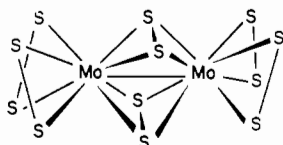
Figure 5. Energy levels of $\text{CpMoTe}_4\text{MoCp}$ as a function of the Mo-Mo distance.

Table II. Triply Bridged L_mME_nML_m Complexes (n = 3; E = S, Cl, SR; M = Cr, Mo, W, Nb)

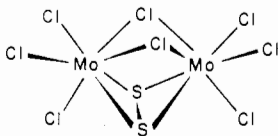
triplely bridged compds	electron count	ref
[Cl ₄ W(μ-Se)(μ-Se ₂)WCl ₄] ²⁻	30	37
[Br ₄ W(μ-S)(μ-S ₂)WBr ₄] ²⁻	30	38
[(C ₄ H ₈ S)Cl ₃ Mo(μ-S ₂)(μ-SC ₄ H ₈)MoCl ₃ (SC ₄ H ₈)] ²⁻	30	39
CpCr(μ-S-t-Bu) ₂ (μ-S)CrCp	30	40
Nb ₂ X ₂ Y ₂ (X = Se, Te; Y = Br, I)	30	43
Mo(S ₂)Cl ₃	30	44
(Me ₂ S) ₂ Cl ₂ Nb(μ-S ₂)SNbCl ₂ (SMe ₂) ₂	30	45a
(C ₄ H ₈ S) ₂ Cl ₂ Nb(μ-S ₂)SNbCl ₂ (SC ₄ H ₈) ₂	30	45b

σ orbitals, which were always filled in the S-bridged compounds 1–3, are not occupied. The all-antibonding tangential a_{2g} (b₂) orbitals, for example, which carried a major part of the destabilization for short S–S distances in 2, are not occupied in 19. In the same manner the e_g set, which is pushed up for short Te–Te distances as well, is empty. Some metal orbitals (δ/δ*) are occupied instead; these are essentially nonbonding for M–M distances of ~3.4 Å. From Figure 5 one would expect a (hypothetical) Te-bridged compound to prefer a structure having Te–Te bonds and long metal–metal separations.

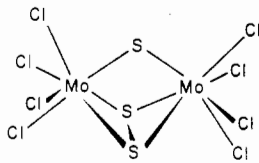
A number of similar sulfur and/or halogen-bridged compounds—molecular as well as solid state examples—have been described. They are compiled in Table I. There is—surprisingly enough—a “magic electron count” for these compounds. Let us take [(S₂)₂Mo(S₂)₂Mo(S₂)₂]²⁻ (22)¹⁶ as an example. Taking the

**22**

terminal S₂ groups as four-electron donors, the skeletal electron count is 34, and this electron count is good for many compounds in that group. Some other compounds, e.g. [Cl₃Mo(μ-S₂)-Cl₂MoCl₃]²⁻ (23),²⁴ have an electron count of 32. This electron

**23**

count is easy to rationalize. We populate or depopulate the b₂ orbitals, which are almost purely metal–metal δ* bonding. Since δ bonds tend to be weak, the Mo–Mo distance is not affected very much. Some related triply bridged compounds, such as [Cl₄WSe₃WCl₄]²⁻ (24),³⁷ which are collected in Table II, have

**24**

(37) Drew, M. G. B.; Fowles, G. W. A.; Page, E. M.; Rice, D. A. *J. Am. Chem. Soc.* **1979**, *101*, 5827.

(38) Klingelhöfer, P.; Müller, U. Z. *Anorg. Allg. Chem.* **1986**, *542*, 7.

(39) Hughes, D. L.; Richards, R. L.; Shortman, C. *J. Chem. Soc., Chem. Commun.* **1986**, 1731.

been reported as well. Here one four-electron donor atom is missing compared to 23, and the resulting electron count is 30. 23, however, is reported to be paramagnetic, S = 1, which is difficult to understand if b₂ is the depopulated level. In order to clarify this discrepancy, we did a calculation on 23 using the experimental geometry. As in other related compounds, there is a HOMO–LUMO gap of approximately 0.6 eV. We are unable to explain the magnetic behavior of this complex from our computations.

Structurally, the quadruply and triply sulfur-bridged early-transition-metal compounds are not very selective. A unifying feature for all of them is a formal metal–metal σ bond. This precludes a fully bonded central ring for geometrical reasons. In comparison to the P₃-bridged compounds L₃MP₃ML₃ (M = Fe, Co, Ni, Pd, Pt),⁴⁷ there seems to be enough “stereochemical power” behind a M–M σ bond to dominate the structure for the early-transition-metal compounds.

We pause here for a moment to recall what we have learned so far. Four-membered rings of main-group atoms sandwiched between metal fragments are rare, and rings of group 16 atoms are—to our knowledge—not known at all. One can blame—as we did in the introduction—the combined constraints of M–L distance, L–L contacts in the bridge, and M–M separation to explain this fact. On the other hand, one can chose a slightly different point of view. As we have shown elsewhere,⁴¹ the interactions of the e₁ hybrids (xz, yz) of the metal fragments with the “lone-pair” orbitals of the central ring becomes an important factor of bonding in inorganic “triple-decker” compounds. More specifically, for different sizes of the central ring there is a competition between a₂''/π (z²/z) and e₁''/lone pair interaction of the metal fragment and the inorganic ring.^{41c} For a six-membered ring the e₁''/lone pair interaction reaches a maximum, whereas the z²/z interaction goes through a minimum. The overlap between the a₂'' combinations of the metal fragment and the inorganic ring, z² and z, respectively, is small, because the atoms of the central ring are situated in the node of the z² orbitals. If the ring size is reduced, then the main-group atoms are moving out of the node. As a result, the corresponding overlap increases. In contrast, the overlap of the e₁'' combinations with the lone-pair orbitals of the ring is diminished. For a three-membered ring, ⟨e₁''|lone pair⟩ reaches a minimum while ⟨z²|z⟩ approaches its

(40) (a) Pasynskii, A. A.; Eremenko, I. L.; Rakitin, Yu. V.; Novotortsev, V. M.; Kalinnikov, V. T.; Aleksandrov, G. G.; Struchkov, Yu. T. *J. Organomet. Chem.* **1979**, *165*, 57. (b) For adducts Cp₂Cr₂(S-t-Bu)₂SML_n (ML_n = Cr(CO)₅, Mn₂(CO)₉) of this structure type see: Pasynskii, A. A.; Eremenko, I. L.; Rakitin, Yu. V.; Orasakhatov, B.; Novotortsev, V. M.; Ellert, O. G.; Kalinnikov, V. T.; Aleksandrov, G. G.; Struchkov, Yu. T. *J. Organomet. Chem.* **1981**, *210*, 377. Pasynskii, A. A.; Eremenko, I. L.; Orasakhatov, B.; Rakitin, Yu. V.; Novotortsev, V. M.; Ellert, O. G.; Kalinnikov, V. T.; Aleksandrov, G. G.; Struchkov, Yu. T. *J. Organomet. Chem.* **1981**, *210*, 385; **1981**, *214*, 351. (c) A series of “bow tie” clusters [Cp₂Cr₂(S-t-Bu)₂S]_nM (M = Cr, Mn, Co) related to the Cp₂Cr₂(S-t-Bu)₂S complexes has been reported as well: M = Cr; Pasynskii, A. A.; Eremenko, I. L.; Orasakhatov, B.; Gasanov, G. Sh.; Shklover, V. E.; Struchkov, Yu. T. *J. Organomet. Chem.* **1984**, *275*, 71. M = Co: Pasynskii, A. A.; Eremenko, I. L.; Orasakhatov, B.; Gasanov, G. Sh.; Shklover, V. E.; Struchkov, Yu. T. *J. Organomet. Chem.* **1984**, *275*, 183.

(41) (a) Tremel, W.; Hoffmann, R.; Kertesz, M. *J. Am. Chem. Soc.*, in press. (b) Jemmis, E. D.; Reddy, A. C. *Organometallics* **1988**, *7*, 1561. (c) Tremel, W. Unpublished results.

(42) (a) Faggiani, R.; Gillespie, R. J.; Campana, C.; Kolis, J. W. *J. Chem. Soc., Chem. Commun.* **1987**, 485. Seigneurin, A.; Makani, T.; Jones, D. J.; Rozière, J. *J. Chem. Soc., Dalton Trans.* **1987**, 2111. (b) A theoretical analysis for O₃ complexes may be found in: Sung, S.-S.; Hoffmann, R. *J. Mol. Sci.* **1983**, *1*, 1.

(43) Franzen, H. F.; Hönl, W.; von Schnering, H.-G. *Z. Anorg. Allg. Chem.* **1983**, *497*, 13.

(44) Marcoll, J.; Rabenau, A.; Mootz, D.; Wunderlich, H. *Rev. Chim. Miner.* **1974**, *11*, 607.

(45) (a) Drew, M. G. B.; Rice, D. A.; Williams, D. M. *J. Chem. Soc., Dalton Trans.* **1984**, 1087. (b) Drew, M. G. B.; Rice, D. A.; Williams, D. M. *Acta Crystallogr., Sect. C: Cryst. Struct. Commun.* **1984**, *C40*, 1547.

(46) DuBois, D. L.; Miller, W. K.; Rakowski DuBois, M. *J. Am. Chem. Soc.* **1981**, *103*, 3429.

(47) (a) DiVaira, M.; Stoppioni, P.; Peruzzini, M. *Polyhedron* **1987**, *6*, 351. (b) DiVaira, M.; Sacconi, L.; Stoppioni, P. *Angew. Chem.* **1982**, *94*, 338; *Angew. Chem., Int. Ed. Engl.* **1982**, *21*, 330.

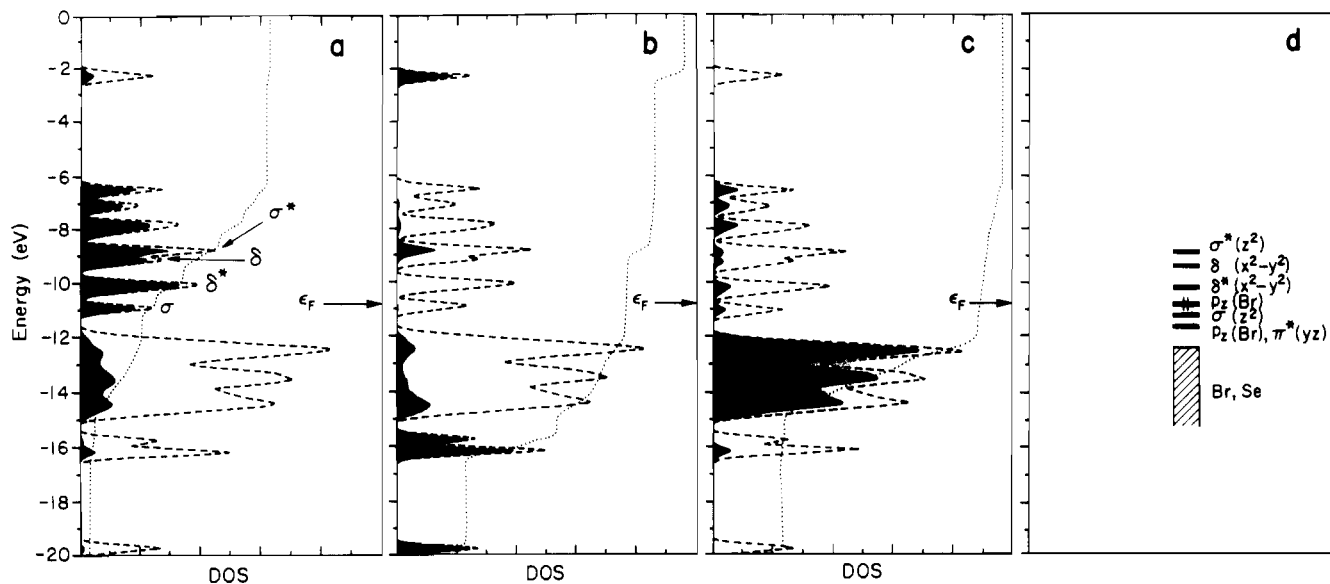
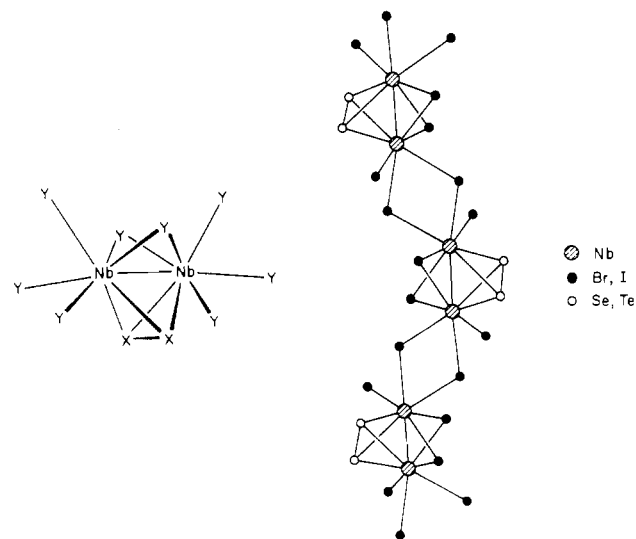


Figure 6. Total DOS (dashed line) and projected DOS (blackened area) for NbSe_2Br_6 giving (a) the Nb, (b) the Se, and (c) the Br contributions. The energy levels of a molecular $[\text{Br}_3\text{NbSe}_2\text{Br}_2\text{NbBr}_3]^{2-}$ unit are shown in (d).

maximum value. The combined overlaps have the smallest value for a four-membered ring, and—as we have seen—for this geometry nature prefers cleavage of the central ring as one possible structural alternative. Whether the central ring breaks or not should be mainly determined by the relative electronegativities of its constituents and the electron count. For S-based systems the electron count of the central ring is large enough that S–S σ bonds are broken. For many P and As type systems, however, the central ring can accommodate the imposed charge and stay intact. Interestingly, $[(\text{CO})_4\text{WTe}_3]^{2+}$, a complex containing a Te_3 ring has recently been made.⁴² This structure supports our hypothesis that Te rings may indeed be stabilized with appropriate metal fragments. In summary, we think that several factors are responsible for the cleavage of the central ring in the title compounds: the relatively small stability of the sandwiched four-membered rings, the electron count, and the presence of a very stable structural alternative, namely a metal–metal-bonded system such as **3**.

We have already mentioned that in the Nb compounds in Tables I and II the (metal–metal) δ^* -bonding orbitals are not occupied. $\text{Nb}_2\text{Se}_2\text{I}_6$ (**25**), an interesting solid-state example, was reported



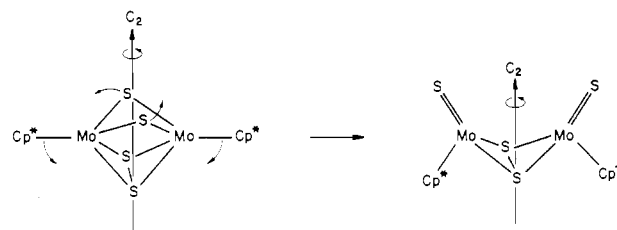
25

by Franzen, Hönlé, and Schnering.⁴³ From the composition one might have expected a Nb^{5+} compound. One finds, however, infinite chains of halogen-bridged $\text{Nb}_2\text{Se}_2\text{I}_4$ units containing Se_2

dumbbells bridging a Nb–Nb bond in a side-on fashion. A number of homologous compounds, $\text{Nb}_2\text{Se}_2\text{Br}_6$, $\text{Nb}_2\text{Te}_2\text{Br}_6$, and $\text{Nb}_2\text{Te}_2\text{I}_6$, could be prepared. Although we find isolated Nb_2 pairs in the structure, all of these compounds exhibit metallic luster and undergo reversible thermal transitions with temperature. Franzen et al.⁴³ speculate that the existence of Nb in a formal 4+ oxidation state and of a chalcogen in an 1– oxidation state permits a simultaneous redox reaction leaving us with niobium(5+) and chalcogen(2–), respectively. This case is in fact closely related to the examples we discussed before, i.e. the transitions between **2** and **3**. From Figure 4 we can see that the reaction is symmetry forbidden. Experimentally, there is no tendency for thermal anisotropy within the Nb_2Y_2 unit.

Since we observe a pairing distortion in this structure, the bonding can be expected to be very localized within the Nb_2Y_2 tetrahedra. We have computed a band structure for the polymer, and it supports this picture. The actual bands are not shown, only the contributions of individual orbitals to the DOS in Figure 6. At –16 eV are—very localized—the Se–Se-bonding states; next come, spread out over some 3–4 eV, the halogen states, mostly lone pairs. Around –11 eV we find the metal states. First is the Nb–Nb σ bond; the next two peaks are the δ and δ^* levels, followed by σ^* . The other δ and the π states are raised by interactions with the other ligands. The DOS projections may be compared with the levels of a $\text{Br}_3\text{Nb}(\text{Se}_2)\text{Br}_2\text{NbBr}_3$ unit in Figure 6d. There is a reasonable match. From our band structure calculations we find in fact a small DOS at the Fermi level (marked with an arrow), indicating (semi)metallic behavior. Substituting Se by Te brings more chalcogen states close to the Fermi level, but the general bonding pattern remains unchanged.

There are still other interesting features of the Mo_2S_4 cores. Wachter and co-workers^{14c} reported the thermal conversion of **3** into **4**. A correlation diagram that we construct for this reaction (assuming the persistence of a 2-fold axis, **26**) shows it to be



26

allowed. So is the interconversion of **2** and **5**. DuBois et al.^{27a} used the same line of thought to explain the different structural

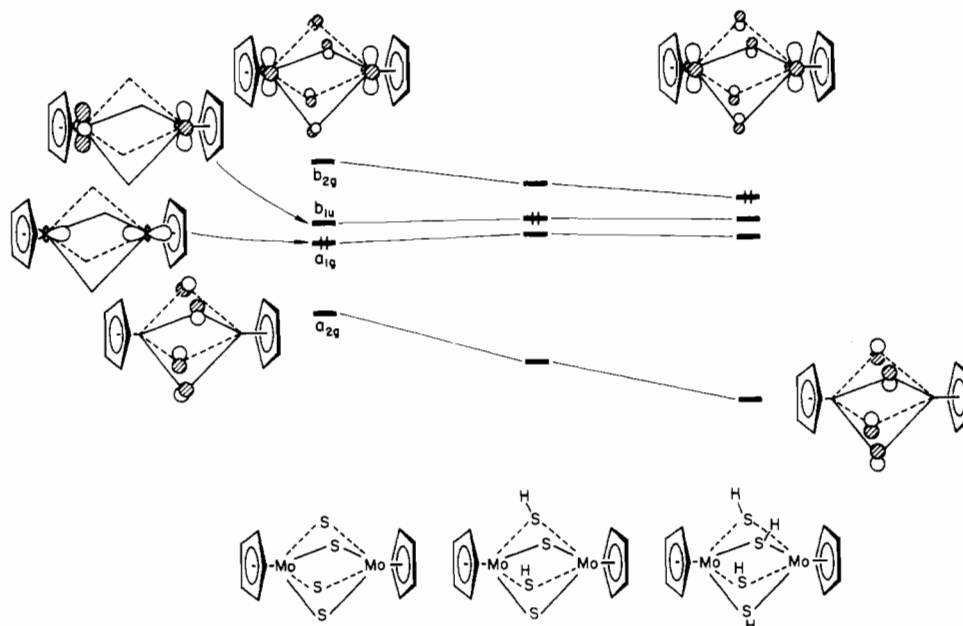
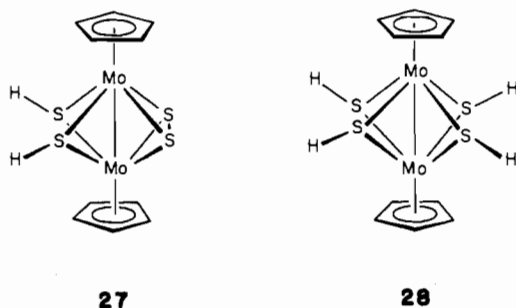


Figure 7. Comparison of the orbital occupancy in CpMoS₄MoCp, CpMo(S)₂(SR)₂MoCp, and CpMo(SR)₄MoCp.

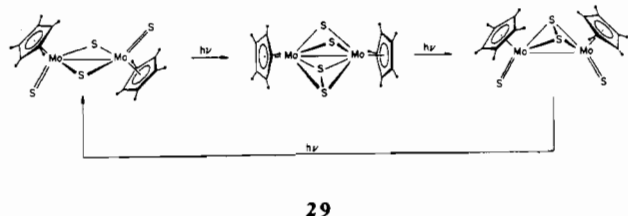
features for the Mo₂S₄ and other known dimers containing different bridging ligands, e.g. 27 and 28.



Perhaps it is worthwhile here to remark on what may be obvious, namely the essential similarity of S²⁻ and SR⁻. SR⁻ is the result, formally (and sometimes actually), of the addition of R⁺ to S²⁻. S²⁻ has four lone pairs, and two are used in bonding to the metals. The third lone pair of S²⁻ is "taken care of" by this maneuver of R⁺ addition. One other one remains, a frontier orbital active in repulsion or further bonding.

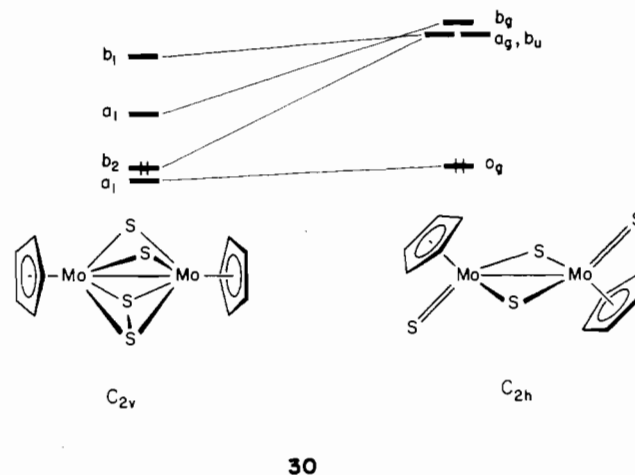
That nothing much happens may be seen in the comparison of the frontier orbitals of 1, 27, and 28 in Figure 7. One must be careful about electron counting: replacing a S by SR without changing the charge on the complex results in a one-electron reduction of the two metals. Therefore, the change in the electron count in Figure 7 results.

It may be interesting to note that a photochemical conversion between structures 3 → 4 → 5 has been reported.⁴⁸ The reaction sequence is given in 29. The isomerization was suggested to result



from a LMCT excited state involving terminal sulfur atoms: Mo is reduced from Mo⁵⁺ to Mo⁴⁺ and S is oxidized from S²⁻ to S₂²⁻. In this process—which is formally a two-electron reduction of the metal—two S²⁻ are transformed into a S₂²⁻ group. One bonding MO is formed; the corresponding antibonding combination is

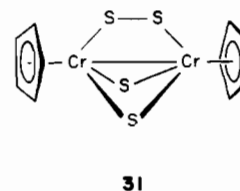
raised in energy. As a result, the b₂ orbital is populated in 3, and in 5 the two electrons are located in a sulfur lone pair. An explanation for the isomerization 3→5 may be gathered from the correlation diagram 30.⁴⁹ The HOMO in 3 is the b₂ orbital. After



the opening process—which is symmetry allowed—a_g is the HOMO of 5. According to our calculations, 5 is preferred for the present electron count.

Moving out of the Central Plane

In the last section we have seen a number of ways in which the sulfur-bridged compounds avoid the formation of a closed *n*-membered ring. The possibilities we found were the breaking of S-S bonds by forming S₂²⁻ groups and S²⁻ ligands or even an η¹-bonding mode of a S₂²⁻ group, as encountered in CpCrS₅CrCp (6).²⁵ Yet there are still other possibilities to escape the ring formation, one of which is realized in CpCr(μ-S)₂(μ-S₂)CrCp (31)⁵⁰ or (*i*-PrCp)V(S₂)₂V(*i*-PrCp) (7).²⁸ The obvious question

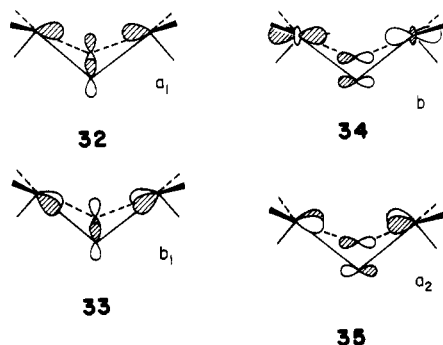


(48) Bruce, A. E.; Tyler, D. R. *Inorg. Chem.* **1984**, *23*, 3433.

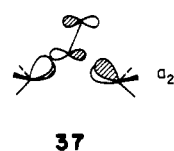
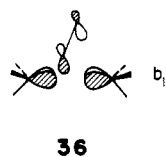
(49) A similar argument has been used to explain the semibringing carbonyls in [CpMo(CO)₂]₂ dimers (M = Cr, Mo): Jemmis, E. D.; Pinhas, A. R.; Hoffmann, R. *J. Am. Chem. Soc.* **1980**, *102*, 2575.

is whether there is an electronic reason for this. The point we address here is related to parallel and perpendicular bonding in acetylene complexes, which has been analyzed by D. M. Hoffman and one of us earlier.⁵¹

In our analysis we can start from the orbitals of a CpV fragment, which were given at the beginning of this paper. Two of these fragments interact. The dimeric CpV...VCp unit will develop into two face-sharing octahedra with the bridging ligands, one S₂²⁻ and two S²⁻. The fragment symmetry is now C_{2v}. We have four filled orbitals on the bridging ligands, which can donate charge into empty orbitals of CpV...VCp. The bonding combinations are shown in 32–35. The frontier orbitals of the

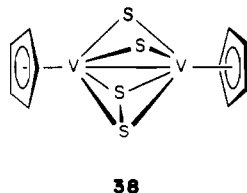


CpVS₂VCp²⁺ fragment are given on the left side of Figure 8. The interaction is illustrated for a S₂²⁻ group in the parallel geometry. The S₂²⁻ group has two π and two π* frontier orbitals. The interaction of the metal fragment with the π orbitals turns out to be not very important, and we focus on the π* metal fragment interactions only. The bonding interactions between π* orbitals of S₂²⁻ and the metal fragment are shown in 36 and 37. From



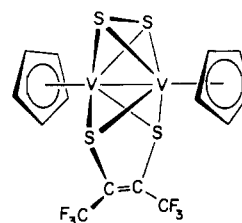
the interaction diagram in Figure 8 we see a gap of approximately 1 eV for a compound with two electrons less. This indicates that species such as CpTiS₄TiCp or CpVAs₂S₂VCp might be kinetically stable. These compounds may be attractive synthetic goals.

For comparison we did a calculation on the "perpendicular" isomer 38. The interaction diagram is not shown here, but in



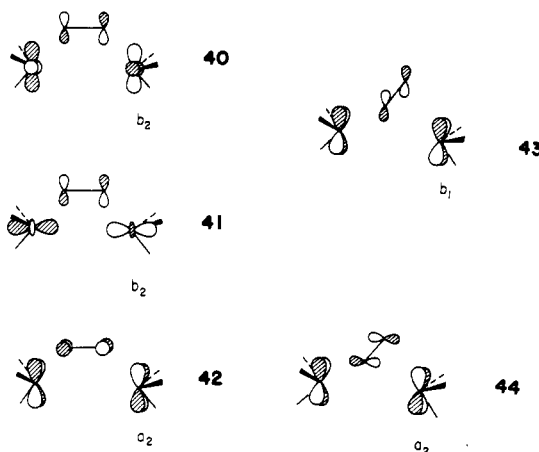
general terms it is not very different from the parallel alternative. The HOMO in both cases represents a M–M σ bond; the LUMO, which is approximately 0.5 eV higher in energy for the parallel geometry, has δ* character. This energy difference for the LUMO could be one reason why—except for 31—compounds with for-

mally two more electrons, i.e. the corresponding Mo compounds or CpV(S₂)(S₂C₂F₆)VCp (39),^{28a} prefer the perpendicular ori-



39

entation. There are some differences in overlap between both structures. By symmetry, in the parallel structure the b₂ orbital can interact with the δ* and σ* combinations of the metal fragment 40 and 41. The a₂ orbital interacts with another δ* com-



bination of the metal fragment 42. The interactions of the π* orbitals in the perpendicular orientation are with the δ(b₁) and δ*(a₂) combinations of the metal fragment 43 and 44.

Our calculations make the perpendicular orientation approximately 0.95 eV more stable than the parallel one. Since the energy matches between the orbitals of bridging S₂²⁻ and the metal fragment are similar, the difference must be caused by the overlap factor. There are two different overlaps to consider in the perpendicular case and three for the parallel bonding mode. Although there are more interacting orbitals in the parallel geometry, the individual overlaps are considerably bigger for the perpendicular S₂ orientation. These differences in overlap are responsible for the energy difference between structures 7 and 38.

If the parallel geometry is less stable by 0.95 eV, why do we not observe the perpendicular geometry, or why do we not have an interconversion between the two structures? As in the case of the acetylene complexes, the reaction is symmetry forbidden. But, given the poor performance of the extended Hückel method in finding a reasonable minimum for the different CpMo₄MoCo isomers 1–3 in Figure 2, is the 0.95-eV energy difference at all credible? As we mentioned above, the main problem in calculating a reliable minimum for 1–3 lies in the presence of several level crossings that make the problem hard to tackle within the framework of the one-electron model. For the conversion 7 → 38 the situation is less complicated. There is a level crossing between the a₂ orbitals, though an avoided one. This leaves us with a diamagnetic species all along the isomerization pathway. Moreover, the interactions responsible for the stability of 7 and 38, the fragment overlaps shown in 40–44 overlaid by a small amount of S...S repulsion, are quite transparent. We think that the energy difference between 7 and 38—even though its absolute numerical value may be not reliable—is significant.

We just mentioned that during the rotation of the S₂²⁻ there is a level crossing between the a₂ orbitals, though an avoided one. If we rotate the S₂ unit in 7, the a₂ orbitals cross-correlate with

(50) Goh, L. Y.; Mac, T. C. W. *J. Chem. Soc., Chem. Commun.* **1986**, 1474.
 (51) (a) Hoffman, D. M.; Hoffmann, R.; Fisel, C. R. *J. Am. Chem. Soc.* **1982**, *104*, 3858. (b) Hoffman, D. M.; Hoffmann, R. *J. Chem. Soc., Dalton Trans.* **1982**, 1471.

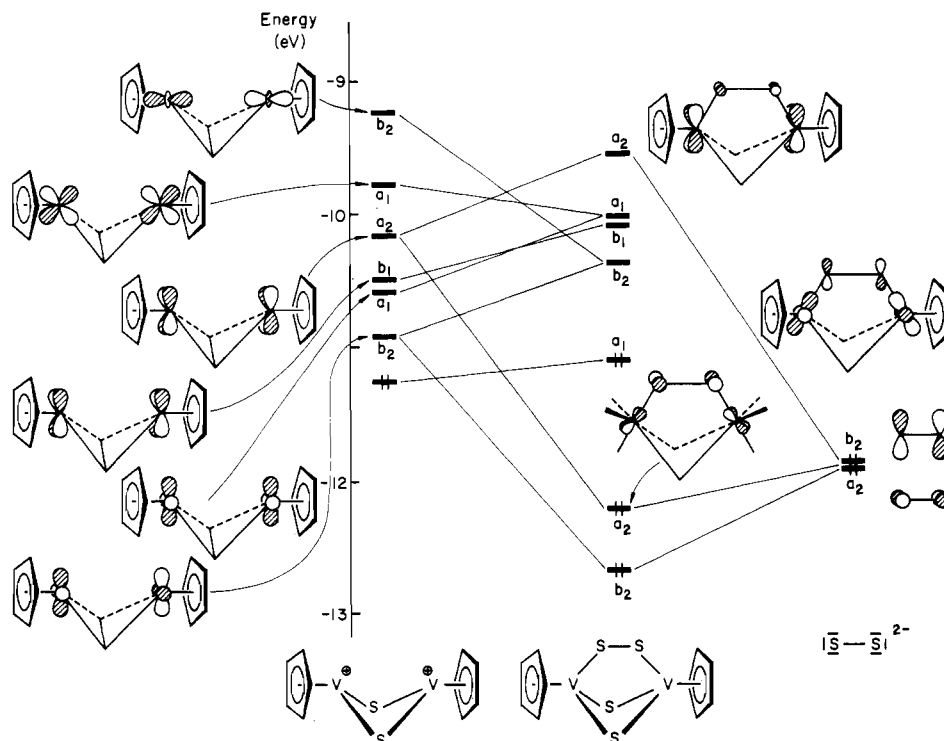
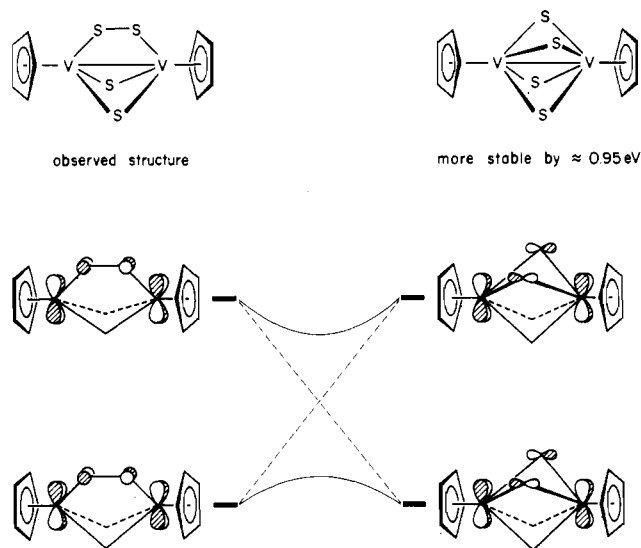


Figure 8. The interaction of $[\text{CpVS}_2\text{VCp}]^{2+}$ with S_2^{2-} in the parallel geometry.

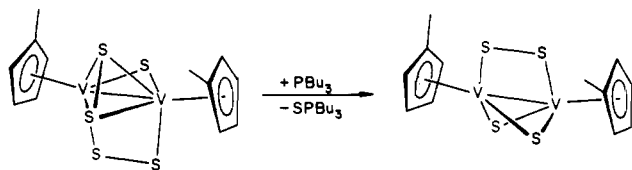
the corresponding orbitals in **38**. We calculated a correlation diagram for the rotation **45**, keeping the V-S distance constant



45

during the motion. No energy barrier was found. We still think it is justified to call the reaction forbidden, because there is an intended level crossing.

If **7** is less stable than **38**, why is it formed at all? The formation of **7** is determined kinetically. Presumably **7** is formed from (*i*-PrCp)₂V₂S₅ (**8**)^{28a} via S abstraction from the μ - η^2 -S₂ unit, **46**.⁵²



46

Table III. Parameters Used in Extended Hückel Calculations

atom	orbital	H_{ii} , eV	ζ_1	ζ_2	C_1^a	C_2^a
S	3s	-20.00	1.817			
	3p	-13.30	1.817			
Te	5s	-20.80	2.51			
	5p	-14.80	2.16			
Cl	3s	-30.00	2.033			
	3p	-15.00	2.033			
Br	4s	-27.01	2.588			
	4p	-12.44	2.131			
I	5s	-23.30	2.681			
	5p	-14.00	2.322			
V	3d	-11.00	4.75	1.70	0.4755	0.7052
	4s	-8.81	1.30			
Cr	4p	-5.52	1.30			
	3d	-11.22	4.95	1.80	0.5060	0.6750
Nb	4s	-8.66	1.70			
	4p	-5.24	1.70			
Mo	4d	-12.10	4.08	1.64	0.6401	0.5516
	5s	-10.10	1.89			
Mo	5p	-6.86	1.85			
	4d	-11.06	4.54	1.90	0.5899	0.5899
Mo	5s	-8.77	1.96			
	5p	-5.60	1.90			

^a These are the coefficients in the double- ζ expansion.

In general, synthetic rationales for most of the compounds we discussed in this paper are hard to give. A typical synthesis starts out from an organometallic precursor that is reacted with elementary sulfur, phosphorus, or arsenic. The product distribution seems to be determined by those fragments of main-group atoms, which are initially cut out of these molecular units (e.g. S₃ rings or P₄ tetrahedra). The energy barriers to excising or abstracting such E_n units must be small. Some day we will understand the mechanisms of formation of these compounds, but for the moment

(52) Similar reactions have been reported, e.g. for the conversion of (MeCp)₂V₂Fe(CO)₃S₄ to (MeCp)₂V₂Fe(CO)₃S₃, and [Mo₃S₇(SCH₂CH₂S)₃]²⁻ to [Mo₃S₄(SCH₂CH₂S)₃]²⁻, respectively. Bolinger, M. C.; Rauchfuss, T. B.; Wilson, S. R. *J. Am. Chem. Soc.* **1982**, *104*, 7313. Halbert, T. R.; McGauley, K.; Pan, W.-H.; Czernuszewicz, R. S.; Stiefel, E. I. *J. Am. Chem. Soc.* **1984**, *106*, 1849. Keck, H.; Kuchen, W.; Mathow, J.; Wunderlich, H. *Angew. Chem.* **1982**, *94*, 927; *Angew. Chem., Int. Ed. Engl.* **1982**, *21*, 929.

we must be satisfied with the partial understanding of the structures themselves, which we think we have attained.

Acknowledgment. We are grateful to the members of our research group for useful discussions. We thank the Deutsche Forschungsgemeinschaft (DFG) and the Verband der Chemischen Industrie for postdoctoral and Habilitation fellowships to W.T. and the NSF for the support of this work under Research Grants CHE 84064119 and DMR 84722702 to the Materials Science Center. Computing equipment at the University of Münster was purchased through a grant by the Deutsche Forschungsge-

meinschaft (DFG, Kr 406/9-1). We are grateful to Jane Jorgensen and Elisabeth Fields for their expert drawings.

Appendix

All the calculations were performed by using the extended Hückel method^{33a,b} with weighted H_{ij} 's.^{33c} Unless otherwise mentioned, the experimental bond lengths were used. The values for the H_{ij} 's and the orbital exponents are listed in Table III. The parameters for C and H are the standard ones.^{33a,b}

Registry No. Mo, 7439-98-7.

Contribution from the Department of Chemistry,
University of Western Ontario, London, Ontario, Canada N6A 5B7

Dependence of Bond Angles upon Bond Distances in Simple Covalent Hydrides, Halides, and Oxides¹

N. Colin Baird

Received August 24, 1988

Ab initio molecular orbital calculations for a variety of hydrides, fluorides, and oxides of first- and second-row elements show that the optimum bond angle subtended by a pair of ligands increases significantly as the internuclear separation between the ligand and the central atom is decreased. This dependence is interpreted in terms of a directed valence theory of bonding, with departures from ideal bond angles arising from steric clashes among ligands. Some of the apparent anomalies of bond angles in simple hydrides and halides are resolved by the discovery that the steric size of a ligand depends significantly upon the length of its bond to the central atom.

For many years, chemists have attempted to elucidate the principal factors that determine the three-dimensional arrangement of ligands X about a central atom A in common molecules. The most successful simple theory of structure is the well-known VSEPR (valence shell electron pair repulsion) method elaborated by Gillespie,² in which repulsion between electron pairs on A is considered to be the dominant factor. In VSEPR, the number of electron pairs at A determines the "ideal" geometry, and the electronegativity of the ligands controls minor deviations from this structure.

We wish to report *ab initio* molecular orbital calculations which indicate that the bond distance R_{AX} is a major factor in determining the optimum XAX bond angle in AX_n molecules, particularly if A is a first-row element.

The variation in HOH angle with changes to the OH bond distance in H_2O is illustrated in Figure 1.³ The MO calculations here use the 6-31G* basis set,^{4,5} i.e., one that includes d orbitals on oxygen, in which inner-shell atomic orbitals are expanded by a fixed linear combination of six Gaussian orbitals and the valence-shell atomic orbitals are expanded as a combination of two sets of Gaussians, one with three components and one with one.

The HOH angle widens appreciably as the OH distance is reduced, becoming greater than the tetrahedral value (109.5°) for OH separations of 0.83 Å or less. As the bond is stretched, the angle closes down toward 90°. Similar results are obtained³ for NH_3 (not shown) and for the singlet state of CH_2 (Figure 1). Although the trend of increasing bond angle with decreasing XH atomic separation is also obtained when X is a second-row atom, the rate of change is only about one-third of that obtained when X is from the first row (see Figure 1 results for H_2S). Again the limiting angle is near 90° for long bond distances but stays well under the tetrahedral value even at short separations. This behavior is not related significantly to the ligand's electronegativity or to the number of lone pairs on A, as the variation for CH_2 is similar to that for H_2O and is very different from that for PH_3 (not shown).

The substantial dependence of bond angle upon interatomic separation and the limiting values of about 90° for bond angles at long separations for the hydrides are unanticipated by VSEPR theory. To explore this point further and to discover the actual reasons for bond angle variations, the *ab initio* MO calculations were extended to a variety of other molecules. For reasons of economy, smaller basis sets were employed.⁷ The basis set used

- Research supported by the Natural Sciences and Engineering Research Council of Canada.
- Gillespie, R. J., *Molecular Geometry*; Van Nostrand Reinhold: Company: London, 1972.
- The detailed values of the predicted bond angles and energies as a function of the varied separations are reported in Tables 1-4, available as supplementary data.
- Hehre, W. J.; Radom, L.; Schleyer, P. v. R.; Pople, J. A. *Ab Initio Molecular Orbital Theory*; Wiley-Interscience: New York, 1986; Chapter 4.
- Calculations were performed on a VAX 8600 using the GAUSSIAN 86 program (release C) from Carnegie-Mellon University, by M. Frisch, J. S. Binkley, H. B. Schlegel, K. Raghavachari, R. Martin, J. J. P. Stewart, F. Bobrowicz, D. Defrees, R. Seeger, R. Whiteside, D. Fox, E. Fluder, and J. A. Pople.

- Calculations with the 6-31G* basis set which include correction for the more substantive effects of electron correlation have been performed by second-order Moller-Plesset perturbation theory. The bond angle-bond length curves are virtually identical with those without correlation when the distances are short. (This applies even to the results for CH_2 , for which there is a doubly excited configuration that lies close to the lowest singlet state.) For long AX separations, the optimum XAX angles are smaller than those obtained by the Hartree-Fock calculations, due to incipient bonding between the ligands themselves that is introduced by incorporating doubly excited configurations into the wave function. For example, as the OH bond in H_2O becomes very long, the best electronic structure eventually becomes an oxygen atom separated from an H_2 molecule. To avoid these difficulties, and because there is no significant effect of correlation upon angle at short AX separations (the area of prime importance here), these 6-31G*/MP2 calculations are not discussed further herein.